Incoherent Detection of Orthogonal Polarizations via an Antenna Coupled MKID Experimental Validation at 1.55 THz

Yurduseven, Ozan; Bueno, Juan; Yates, Stephen; Neto, Andrea; Baselmans, Jochem; Llombart, Nuria

DOI
10.1109/TTHZ.2018.2873890

Publication date
2018

Document Version
Accepted author manuscript

Published in
IEEE Transactions on Terahertz Science and Technology

This article has been accepted for publication in a future issue of this journal, but has not been fully edited. Content may change prior to final publication. Citation information: DOI 10.1109/TTHZ.2018.2873890, IEEE Transactions on Terahertz Science and Technology

Incoherent Detection of Orthogonal Polarizations via an Antenna Coupled MKID: Experimental Validation at 1.55 THz

Ozan Yurduseven, *Member IEEE,* Juan Bueno, Stephen Yates, Andrea Neto, *Fellow Member, IEEE,* Jochem Baselmans and Nuria Llombart, *Senior Member, IEEE*

***Abstract*— There is an increasing demand for large format detector arrays with large bandwidths and high antenna efficiencies for future THz astronomical radiometric applications. For direct detection instruments, it is also desired to have antennas with dual polarization reception in order to increase the received power from incoherent sources, thereby improving the observing speed of the instrument. The main goal of this work is the validation of the incoherent detection of two orthogonal polarizations by a leaky lens antenna, coupled to a single Microwave Kinetic Inductance Detector (MKID). Depending on the absorbed power over a distributed transmission line, the resonant frequency of the MKID changes. The proposed antenna is composed of two crossed leaky wave slots feeding a silicon extended hemispherical lens. The slots are coupled to four aluminum (Al) coplanar waveguide (CPW) lines that incoherently absorb the incoming THz radiation. The antenna and the power absorbing CPW lines are embedded inside the MKID, allowing an efficient radiation detection at THz frequencies where no lossless superconductors are available. The proposed dual-polarized device absorbs power incrementally over four different CPWs incoherently and is therefore simulated in reception (deriving a plane-wave response) similarly to what is done in distributed absorbers. We compare numerically and experimentally the proposed dual-polarized leaky lens coupled MKID and its single polarization counterpart and show that the dual polarized device receives twice as much power as the single-polarized one. Eventually, the dual-polarized device, when used with air-bridges, provides the same angular selectivity and twice the throughput of the single-polarized one.**

***Index Terms*—dual-polarization, incoherent detectors, lens antennas**

I. Introduction

The next generation mm and sub-mm wave instruments systems for astronomy and cosmology include wide-field mapping with large-FoV survey telescopes and deep mapping from large-aperture, small FoV, telescopes such as the Large Millimeter Telescope (LMT). For space applications, efficient radiation coupling at super THz frequencies is needed in combination with extremely high sensitivities and dual polarized radiation detection [1]. Additionally, Focal Plane Arrays (FPAs) with thousands of detectors are required. Microwave Kinetic Inductance Detectors (MKIDs), originally proposed by Day *et. al*. in 2003 [2], have allowed the construction of large scale, mm-wave imaging instruments with high multiplexing factors and limited complexity and cost. A good example is the lumped element KID based NIKA2 instrument on the IRAM 30m telescope [3]. For the highest sensitivities and sub-mm/THz instruments the lens-antenna coupled MKID's have the advantage that the radiation coupling and the detector sensitivity can be optimized independently. The most widely used configuration is the double slot antenna coupled MKID, which typically operates over a narrow bandwidth with a single polarization. An example is the device described in [4] that operates at 850 GHz with extremely high sensitivities, achieving a measured noise equivalent power (NEP) of $\approx 3 \times 10^{-19}\,\mathrm{W}/\sqrt{\mathrm{Hz}}$. A 961 pixel detector was constructed based upon this device with an identical sensitivity [5] using a dedicated microwave readout system to read-out all detectors simultaneously using frequency division multiplexing at microwave frequencies [6]. This system meets the sensitivity requirement for future imaging instruments on board of a space-based observatory with a cryogenically cooled telescope, such as SPICA-SAFARI and the Origins Space Telescope (OST). However, it operates at a limited bandwidth and low frequency. The aforementioned observatories will require detectors operating in the 1-10 THz frequency band, and, for SPICA-SAFARI, an input bandwidth of about one octave: for example, the low frequency band from SAFARI is defined from 1.4 THz to 2.7 THz [7]. For such wide bandwidths, log spiral [8] or sinuous antennas [9] based lenses, [10] have been proposed, but they are difficult to fabricate with distributed feeding lines at

This Manuscript received Month DD, YYYY; revised Month D,D YYYY. First published Month DD, YYYY; current version published Month DD, YYYY. This work was supported by ERC Starting Grant ERC-2011-StG Grant Advanced Antenna Architectures for THz Sensing Instruments (AAATSI), No. 278794 and as part of a collaborative project, SPACEKIDS, funded via grant 313320 provided by the European Commission under Theme SPA.2012.2.2-01 of Framework Programme 7. The work of Nuria Llombart was supported by the ERC Starting Grant LAA-THz-CC (639749). The work of J. J. A. Baselmans was supported by the ERC consolidator Grant COG 648135 MOSAIC.

O. Yurduseven, N. Llombart Juan and A. Neto are with the Microelectronics Department of the EEMCS Faculty, Delft University of Technology, 2628 CD Delft, The Netherlands (e-mail: N.LlombartJuan@tudelft.nl).

J. Bueno and J. J. A. Baselmans are with SRON Netherlands Institute for Space Research, Utrecht, 3584 CA, The Netherlands.

S. Yates is with SRON Netherlands Institute for Space Research, Groningen, 9747AD The Netherland.

This article has been accepted for publication in a future issue of this journal, but has not been fully edited. Content may change prior to final publication. Citation information: DOI 10.1109/TTHZ.2018.2873890, IEEE Transactions on Terahertz Science and Technology

such high frequencies. Recently a leaky slot based antenna solution was proposed providing a bandwidth up to 1:10 at a frequency range of 0.15 – 1.5 THz with a very good agreement between the simulated and measured antenna beam patterns [11]. Improving the lens illumination efficiency and changing the detector materials has led to a single polarized THz version of the leaky-lens antenna coupled KID [12] with a bandwidth of an octave. A photograph of this device is shown in Fig.1a.

All these previous antenna concepts receive only a single polarization from an incoherent source. The reception of two orthogonal linear polarizations will further increase the sensitivity. To this end a dual-polarized leaky lens based solution was proposed in [13].

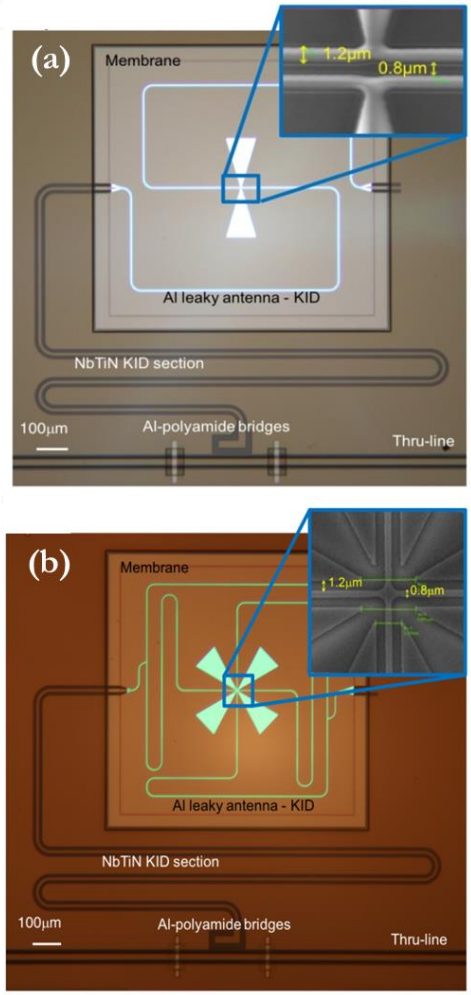

Fig. 1. Photographs of the fabricated single (a) and dual-polarized (b) leaky slot coupled KID devices.

In this contribution, we present the simulated and measured angular response and normalized optical throughput of a dual-polarized leaky-wave coupled MKID, shown in Fig1b, and compared it to its single-polarized version. We show, experimentally and theoretically, that the dual polarized device absorbs twice the amount of power from an incoherent, thermal calibration source than its single-polarized version. We will also show that the dual polarized detector receives the power in four different coplanar waveguide (CPW) lines incoherently. To be able to do this we analyze the detector response and beam pattern in reception via a plane wave illumination, similarly to what is presented in [14] for distributed absorbers. Using this analysis, we show that the moderate directivity of the current device can be fully mitigated by using air-bridges over the four absorbing CPW lines.

The paper is organized as follows: In Section II, we briefly describe the design parameters of the single and dual- polarized leaky lens-antenna coupled MKIDs and present the simulated angular response and simulated normalized optical throughput of the single and dual-polarized detector designs. The single-polarized device is used later in the text as a benchmark for the performance comparison. Section III describes the design and fabrication of the lens-antenna coupled MKID. Section IIV explains the measurement setup used to evaluate the device performances briefly and describes the measurement results performed at 1.55 THz to validate the plane wave response of the dual-polarized detector, the estimated throughput and the factor of two increased in detected power with respect to the single polarized device. The conclusions and the future improvements are given in Section V.

II. Antenna Optical Performance

The dual-polarized antenna is a replica of the configuration presented in [13] scaled to a frequency band from 1.4 THz to 2.8 THz and coupled to two orthogonal CPW lines instead of micro-strips. The choice for planar CPW lines is motivated by fabrication constraints. The dielectric required for hosting a micro-strip would introduce a high loss and noise in the MKID degrading its performance at these frequencies.

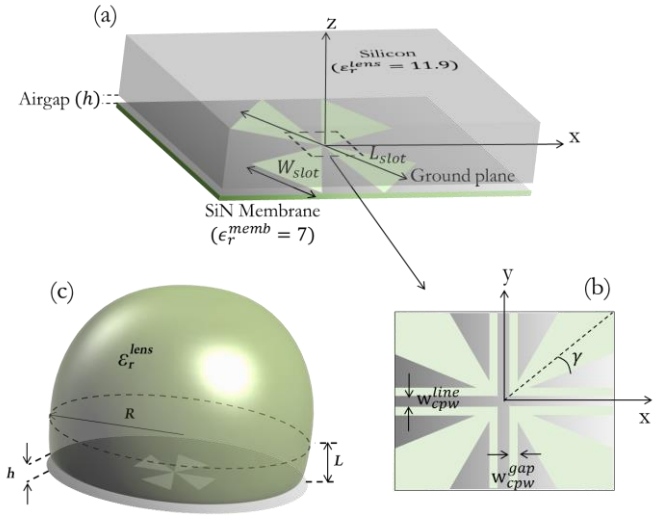

Fig. 2. (a) Geometrical design parameters of the dual-polarized leaky antenna together with the CPW lines. (b) Zooming into the center of the crossing slots and whereas (c) shows the design parameters of the integrated silicon lens

A sketch of the dual-polarized leaky antenna geometry can be seen in Fig.2a, whereas Fig.2b shows the crossing slots and the CPW lines whereas. The entire structure is fabricated from a 75 nm thick layer of aluminum on top of a 1 μm membrane of SiN with a dielectric permittivity of 7. Fig.2c shows the integrated extended hemispherical silicon lens with its geometrical parameters. The lens is coated with a parylene layer

($\varepsilon_r = 2.7$) of thickness h_m. The antenna geometrical parameters are summarized in TABLE I. The slot dimensions are set by the combination of i) the minimum dimensions possible in our fabrication process, ii) the lowest radiation loss, and iii) a good impedance match to the antenna port impedance.

TABLE I
GEOMETRICAL DIMENSIONS OF THE DUAL-POLARIZED ANTENNA

Parameter	Dimension	Parameter	Dimension
L_{slot}	0.602 mm	w_{line}^{cpw}	1.2 μm
W_{slot}	0.173 mm	$s_{airbridge}$	15 μm
γ	15^0	R	1.55 mm
h	6 μm	L	0.31R
w_{gap}^{cpw}	0.8 μm	h_m	23 μm

A. Detector Plane Wave Response

We first start with the evaluation of the angular response of the single-polarized and dual-polarized leaky lens antennas. The schematics of the simulated antenna geometries are shown in Fig.3. The single-polarized leaky slot antenna consists of only one slot and it has been simulated in transmission using CST MWS [15] since it is a single mode antenna. Therefore, it can be modeled using a lumped port located at the center of the slot, exciting an equivalent current distribution associated with only the differential CPW mode (the common mode will only alter the cross-polarization at large angles as shown in [11]). The dual-polarized device, on the other hand, is composed by two crossing leaky slots together with two crossing CPW lines (Fig.2b). We simulate the dual-polarized device in reception by means of launching plane waves with different incidence angles up to $\theta = 20$ deg with a step of $\Delta\theta = 2.5$ deg in four φ-cuts. Each (θ, φ) point includes two orthogonal polarized plane waves, p_1 and p_2, with the same amplitude E_0. After each CST simulation, we calculate the total power absorbed in all the central lines of the four CPW's combined, $P_{abs,CPW}^{p_i}$. The central lines are simulated with the measured sheet resistance of the actual 75 nm thick aluminum film ($\rho_s = 1.125\ 10^{-8}\ \Omega m$, Rs = 0.15 Ω). The total length of each CPW line is 1.25 mm[1], long enough to absorb all THz power. Power absorbed in the ground plane will not be sensed by the MKID detector and is therefore treated as loss.

We evaluate the angular power pattern, $F_n(\theta, \varphi)$ [14] of the antenna coupled detector by repeating this step for all incident angles. The angular power response is normalized to the power absorbed in CPW lines for the broadside plane wave incidence and can be evaluated as follows:

$$F_n(\theta,\varphi) = \frac{P_{abs,CPW}^{p_1}(\theta,\varphi) + P_{abs,CPW}^{p_2}(\theta,\varphi)}{P_{abs,CPW}^{p_1}(0,0) + P_{abs,CPW}^{p_2}(0,0)} \quad (1)$$

[1] The CPW lines have been simulated with a slightly different resistance and a shorter length than fabricated. The length in the simulation was chosen to reach a -10dB power absorption and reduce the simulation time.

Figure 4a shows the comparison of the angular responses obtained from single-polarized leaky (SPL) lens evaluated in Tx (transmission), shown by the solid curves, and the dual-polarized leaky (DPL) antenna coupled KID device evaluated in Rx (reception), shown by dots, in four ϕ-planes. As it can be seen from the figure, although the beams along the slot axes ($\varphi = 45, 135$ deg) are comparable between the single and dual-polarized devices, the dual-polarized patterns have significantly wider beam response than the single-polarized ones on the axes defined along KID lines ($\varphi = 0, 90$ deg). The difference is due to the fact that the dual polarized device responds incoherently to both the common and differential modes that can propagate in the CPW. The effect becomes more significant for larger angles. In order to reduce this effect, we simulated the same geometry but including metallic air-bridges [16] along the CPW lines, as highlighted in Fig.3c. The angular beam response including the air-bridges for the dual-polarized antenna is shown in Fig. 4b. With the suppression of the common mode via the air-bridges, the angular responses of the single- and dual-polarized devices become similar in all φ-planes.

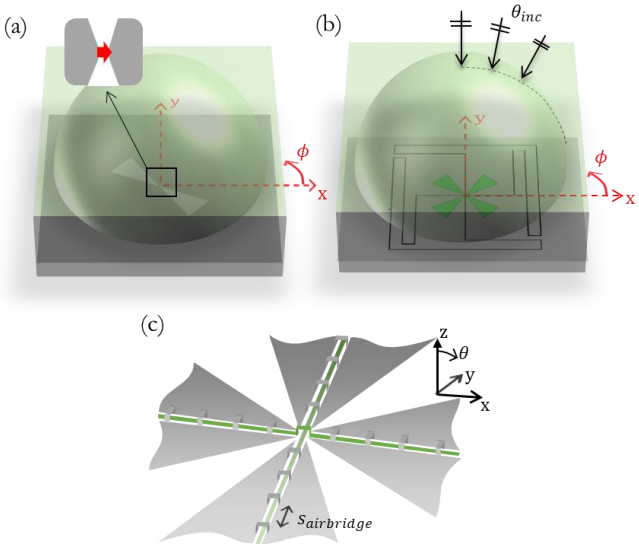

Fig. 3 Schematic of the simulated structures. (a) the single-polarized leaky lens, which is simulated in transmission using the lumped port as indicated. (b) the dual-polarized leaky slot lens antenna coupled KID device simulated in reception. We use the power absorbed in the aluminum CPW lines directly to calculate both the beam pattern as well as the coupling efficiency, for details see the text. The CPW lines together with the air-bridges are highlighted in (c).

B. Normalized Optical Throughput

The spectral power absorbed by a detector from a distributed incoherent source with a source dimension Ω_s and an average temperature of T_s can be calculated as follows:

$$P_{abs}^{T_s}(\nu) = B(\nu, T_s) H(\nu)\, A_{eff}(\nu)$$

This article has been accepted for publication in a future issue of this journal, but has not been fully edited. Content may change prior to final publication. Citation information: DOI 10.1109/TTHZ.2018.2873890, IEEE Transactions on Terahertz Science and Technology

$$\int_0^{2\pi}\int_0^{\theta_s} F_n(\nu,\theta,\phi)sin\theta d\theta d\phi \qquad (2)$$

where $B(\nu,T_s)=\frac{\nu^2}{c^2}\frac{2h\nu}{e^{\frac{h\nu}{k_BT_s}}-1}$ is the source Brigthness with k_B being the Boltszmann's constant and h is Plank's constant, $H(\nu)$ is the transmission coefficient of the filter stack, $A_{eff}(\nu)=A_{lens}\eta_{ap}(\nu)$ is the effective area of the detector, and $F_n\ (\nu,\theta,\varphi)$ the normalized antenna angular response as defined in (1). After some algebraic steps and introducing the efficiencies described in [14] and summarized in (5-7 below), (2) becomes:

$$P_{abs}^{T_s}(\nu)=B(\nu,T_s)\lambda^2H(\nu)\ \frac{\eta_{ap}(\nu)\eta_{so}(\nu)}{\eta_f(\nu)} \qquad (3)$$

where the last term in the equation:

$$\frac{A\Omega}{\lambda^2}=\frac{\eta_{ap}(\nu)\eta_{so}(\nu)}{\eta_f(\nu)} \qquad (4)$$

is referred as normalized throughput or number of the modes of the system [17] (note that in this definition $\frac{A\Omega}{\lambda^2}$ will be equal to 0.5 and 1 for a single and dual polarized antenna, respectively). The definition in (4) is valid for any kind of absorber or antenna. For single mode and single polarized antenna, this normalized throughput becomes $A\Omega/\lambda^2=\frac{1}{2}\eta_{rad}\eta_{so}$ as described in [14], [4], except for the fact of 2. Therefore, in [4], [13] and [18] the term $\frac{A\Omega}{\lambda^2}$ is called the optical coupling efficiency η_{op} since it is always smaller than 1. In case of multi-mode detectors, the normalized throughput can be larger than one [14], which makes the use of the term optical efficiency improper.

The three key detector efficiencies in (4) can be evaluated from the CST plane wave simulations described previously as follows:

- The *antenna aperture efficiency*, which relates the power absorbed at broadside to the incident power, can be evaluated as follows

$$\eta_{ap}=\frac{P_{abs,CPW}^{p_1}(0,0)+P_{abs,CPW,}^{p_2}(0,0)}{P_{in}} \qquad (5)$$

Where $P_{in}=2\frac{|E_0|^2}{2\zeta_0}A_{lens}$ with $A_{lens}=\pi R_{lens}^2$. Here ζ_0 is the free space wave impedance. The factor 2 in P_{in} is included because $P_{abs}^{T_s}$ in (3) is defined using the Brightness expression for two polarizations. This results in a maximum aperture efficiency of 1 for an antenna with 2 polarizations, and ½ for one with a single polarization.

- The *antenna focusing efficiency*[2], which evaluates the enlargement of the angular response of the detector with respect to a diffraction limited beam, can be evaluated as follows:

$$\eta_f=\frac{\lambda^2}{A_{lens}}\frac{1}{\int_0^{2\pi}\int_0^{\frac{\pi}{2}}P_n(\nu,\theta,\phi)sin\theta d\theta d\phi} \qquad (6)$$

- The *aperture spill over efficiency*, which evaluates the ratio of power coupled to the solid angle defined by the measurement setup (see [4]), is evaluated as follows:

$$\eta_{so}=\frac{\int_0^{2\pi}\int_0^{\Omega_s}P_n(\nu,\theta,\phi)sin\theta d\theta d\phi}{\int_0^{2\pi}\int_0^{\frac{\pi}{2}}P_n(\nu,\theta,\phi)sin\theta d\theta d\phi} \qquad (7)$$

It is important to note that all these efficiencies are evaluated using a reception analysis in case of multi-mode detectors.

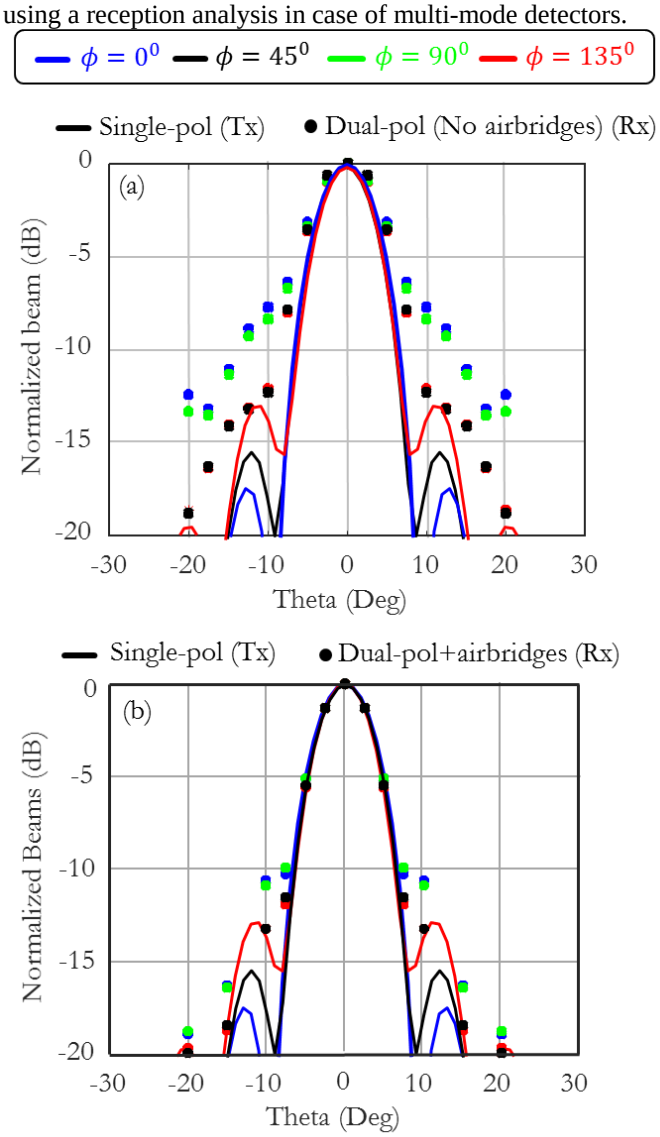

Fig. 4. (a) Comparison of the angular beam responses of the single polarized leaky (lines) and dual-polarized leaky (without air-bridges) lens antennas (dots). (b) The same comparison of the angular beam responses of the single polarized leaky (lines) and dual-polarized leaky lens antenna (dots), but now with air-bridges

We report the estimated values of these efficiencies and throughput in TABLE II for two source apertures with a solid

[2] This efficiency is commonly named taper efficiency when a transmission analysis approach is used.

This article has been accepted for publication in a future issue of this journal, but has not been fully edited. Content may change prior to final publication. Citation information: DOI 10.1109/TTHZ.2018.2873890, IEEE Transactions on Terahertz Science and Technology

angle of $\Omega_s = 3.6^0$ and $\Omega_s = 17.5^0$ associated with the measurement setup. This setup will be discussed in detail in section IV. The throughput has been calculated for the single-polarized device as well as the dual-polarized device with and without the air-bridges.

According to our estimations the normalized throughput for the small angle setup is about 0.07 and 0.15 for the single and dual-polarized devices, respectively. Therefore, this result shows that the received power is twice as much for the dual-polarized device. However, for the large angle setup, one can see that the difference in throughput between the two designs is much larger (0.19 for the single-polarized and 0.64 for the dual-polarized designs). This difference is due a wider angular pattern in case of the dual-polarized antenna as highlighted in Fig. 4a. It is important to note that the aperture efficiency, except for the factor of 2 due to the polarization, is similar for both configurations whereas the focusing efficiency and the spill-over efficiencies are significantly different. This is expected since the absorption of the common mode for the dual-polarized device enlarges the angular beam absorption which, in the end, leads to a worsened focusing efficiency. Including the air-bridges into the dual-polarized device suppresses the common mode, and as a result the angular responses obtained from the single-polarized device in Tx and dual-polarized device in Rx match quite nicely (see Fig. 4b). Hence, they also provide similar focusing efficiencies without changing the aperture efficiency. As a result, the dual-polarized detector with air-bridges presents double throughput values for any source angles compared to the single-polarized device. Basically, the dual polarized antenna leads to the incoherent summation of the power received by two orthogonal single mode linear polarized antennas.

TABLE II
COMPONENTS OF THE SIMULATED NORMALIZED OPTICAL THROUGHPUT OF THE EXPERIMENTAL SETUP AT 1.55 THZ

Single polarized leaky (Tx)				
Ω_s	η_{ap}	η_f	η_{so}	$A\Omega/\lambda^2$
$\mathbf{3.6^0}$	0.155	0.66	0.31	**0.07**
$\mathbf{17.5^0}$			0.80	**0.19**

Dual-polarized leaky (Rx) (Without air-bridges)				
Ω_s	η_{ap}	η_f	η_{so}	$A\Omega/\lambda^2$
$\mathbf{3.6^0}$	0.28	0.42	0.22	**0.15**
$\mathbf{17.5^0}$			0.94	**0.64**

Dual-polarized leaky (Rx) (With air-bridges)				
Ω_s	η_{ap}	η_f	η_{so}	$A\Omega/\lambda^2$
$\mathbf{3.6^0}$	0.28	0.69	0.32	**0.13**
$\mathbf{17.5^0}$			0.96	**0.39**

The value of the aperture efficiency is, for a single moded device, given by the product between the radiation and focusing (taper) efficiencies [18], except for the polarization factor 2. In the proposed single-mode device the value of the radiation efficiency is only 47%. This efficiency is composed of the terms described in TABLE III: the reflection efficiency due to the dielectric-air interface on the lens, η_{ref}^{CST}, the antenna input impedance mismatch efficiency η_{match}, the efficiency associated to the power dissipation in the antenna ground plane (GP) η_{GP} and the CPW radiation losses, η_{CPW}, estimated using the tool described in [19]. Note that power absorbed in the ground plane creates quasiparticles that will diffuse away from the narrow CPW, resulting in a negligible device response. More details are given in Section III. It is important to note that most of these terms are limited by the fabrication constraints and can be improved significantly by using an optimum matching layer, improved antenna impedance matching and CPW radiation losses by fabricating narrower CPW lines, and using a thick ground plane and a thin central CPW line to decrease the percentage of power dissipation in the ground plane [20].

TABLE III also includes the estimated radiation efficiency after these improvements. Based on our estimations, the optimum device would be able to achieve a radiation efficiency larger than 80% which is similar to the radiation efficiencies reported in [4]. Such an efficiency is possible over bandwidths larger than an octave using an advanced, multi-layer AR coating on the lens surface which has to be developed. The same improvement factor (~1.8) in the aperture efficiency of the dual polarized antenna with air-bridges is expected.

TABLE III
COMPONENTS OF THE SINGLE-POLARIZED LENS ANTENNA RADIATION EFFICIENCY AT 1.55 THZ

Radiation efficiency (η_{rad})		
	Current design	Improved design (Estimated)
η_{ref}	0.84	0.94
η_z	0.87	0.99
η_{GP}	0.73	0.9
η_{CPW}	0.88	0.99
η_{rad}	**0.47**	**0.83**

III. KID DESIGN AND FABRICATION

The KID design and fabrication follow the same principles for both the single polarized and dual polarized antennas. The fabrication is described in great detail in [12] for the single polarized version, here we give a summary of the most important steps and parameters.

We fabricate the device on a high resistivity FZ <100> intrinsic Si wafer (ρ > 5kΩcm) coated on both sides with a 1 μm thick SiN layer, which is deposited using low pressure chemical vapor deposition, LPCVD. This SiN layer has a built-in tensile stress of a few hundred MPa, which ensures a stretched, flat SiN membrane. Several lithographic steps allow

This article has been accepted for publication in a future issue of this journal, but has not been fully edited. Content may change prior to final publication. Citation information: DOI 10.1109/TTHZ.2018.2873890, IEEE Transactions on Terahertz Science and Technology

us to create the required stratification with a bare Si substrate for most of the resonator and a free-standing membrane for the antenna feed and narrow CPW lines coupled to the antenna.

The KID is designed as a coplanar waveguide (CPW) resonator, open ended near the feedline and shorted at its far end where the antenna is located. The MKID itself is a $\lambda_{eff}/4$ resonator, where λ_{eff} is the effective wavelength of the readout signal. The length of the KID is about 8 mm which corresponds to a resonant frequency of about 3.5 GHz. The resonator has a quality factor that is controlled by the coupler design. Optical micrographs of both the fabricated single-polarized and the dual-polarized leaky slot antenna coupled KIDs are shown in Fig. 1a and b, respectively. Most of the device consists of a CPW line (linewidth = 8 μm, gapwidth = 12 μm), etched into a 350 nm thick NbTiN film. The NbTiN is deposited using reactive magnetron sputtering on bare Si. The large width and Si substrate reduces device intrinsic noise [21], [22]. The antenna and narrow CPW lines responsible for THz absorption are fabricated from a 75 nm thick aluminum film, sputter deposited on the SiN membrane. The aluminum has a sheet resistance in its normal state of 0.18 Ω and the CPW lines are 1.25 mm long from the antenna feed (i.e. 2.5 mm in total). Radiation absorbed in the aluminum CPW lines near the antenna (both in the central line and the ground plane) will create so-called quasi-particle excitations by breaking Cooper pairs from the superconducting ground state. The result is a change in complex surface impedance of the aluminum, which change in resonant frequency and Q factor of the resonator. This is read out by measuring the forward transmission of the readout line S21, at the resonant frequency. It is important to realize that quasiparticles are mobile and can diffuse through the aluminum. As a result, quasiparticles created in the CPW ground plane diffuse away from the CPW, and thereby away from the microwave currents associated with the readout. Hence, they do not cause a response of the detector. The diffusion of quasiparticles along the CPW lines is controlled by the NbTiN, which has a (much) higher critical temperature (15 K) than the aluminum (1.25K). As a result, the NbTiN creates a 'mirror' for quasiparticles, trapping them in the aluminum. Note that we cannot use NbTiN for the antenna and MKID ground plane of the narrow CPW lines as was done in [4], [5] for devices operating at 850 GHz. The gap frequency of NbTiN is ~1.1 THz, for signals exceeding this frequency NbTiN acts as an efficient absorber. As a result a large fraction (~30%) of the THz power will be absorbed in the NbTiN where it does not contribute to the MKID response[3].

For the single polarization device, the only modification from a simple $\lambda_{eff}/4$ CPW resonator is the addition of the leaky slot in the center of the narrow, aluminum CPW section of the MKID. This adds a little inductance at the readout frequency, reducing the MKID resonant frequency, which is compensated for in the design. For the dual polarized device, the KID CPW line is split up into 2 lines, each in total also 2.5 mm long, to absorb the radiation coming from both polarizations of the antenna. Close to the shortened end of the resonator both lines are combined again. An electromagnetic simulation of the resonator at its readout, resonant frequency, performed with Sonnet, is shown in Fig.5. The 3-way splitters in the resonator are not equipped with vias or air-bridges, which results in a 'floating' ground. The result is a non-symmetric microwave current profile around the separated lines, reducing the responsivity of the MKID. It is important to realize that for the THz radiation reception the narrow CPW's are so long that no THz power remains upon reaching the 3-way splitters, making them irrelevant to the THz radiation. Furthermore, we do not suffer from reflections since the entire structure is a $\lambda_{eff}/4$ resonator, any reflections will cause resonances only at (much) higher frequencies.

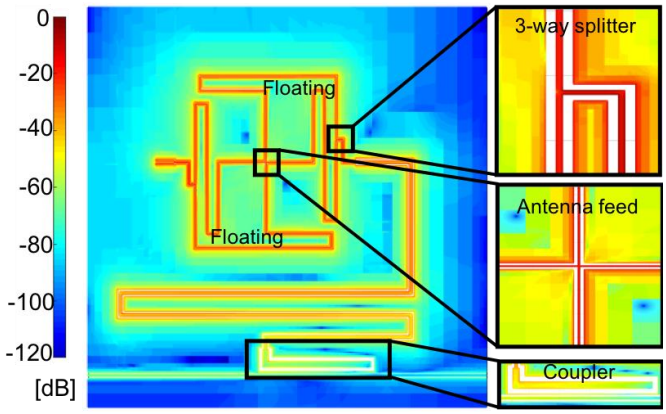

Fig. 5 Electromagnetic simulation at 3.5GHz of the KID read-out resonator.

The leaky wave antenna has a 6 μm vacuum gap between the antenna feed and the dielectric lens. To realize this, we mount the chip in a sample holder and place a spacer wafer on top of the device, which has the function to create the required gap to the antenna feed. On top of the spacer wafer we place the lens, electromagnetically the spacer wafer and antenna form a single unit. Alignment of the assembly is guaranteed using alignment pins, the assembly is kept in place using springs. All details about the fabrication and assembly of this device are explained in [12].

IV. Experimental Results

We describe in this section the measurement results of the dual-polarized leaky device in terms of angular response and the normalized throughput to a distributed incoherent black body source at 1.55 THz. The results are then compared to the numerical results reported in Section II.

We first start with the evaluation of the angular response of the device, which requires direct access from the chips to the 300 K lab environment, which is done using the same setup as described in [4]. The sample is mounted on the cold stage of a He^3 sorption cooler, reaching 300 mK. The optical access consists of a 300K HDPE window, Gore-Tex infrared blockers

[3] NbTiN has an exceedingly short quasiparticle lifetime due to its high critical temperature. Hence, the quasiparticle density, and with that the change in surface impedance, is negligible under constant power absorption.

This article has been accepted for publication in a future issue of this journal, but has not been fully edited. Content may change prior to final publication. Citation information: DOI 10.1109/TTHZ.2018.2873890, IEEE Transactions on Terahertz Science and Technology

and metal mesh low pass filters at 77K and 4K. The apertures on the 77K and 4K stages limit the total angular throughput of the radiation to an opening angle of ±27.5 degree. We illuminate the chip with a ~1000°C black body radiator with a small aperture, mounted on a XY scanner that allows us to measure the MKID response as a function of the source position. Further information of the measurement setup can be found in [4].

Figure 6**Fout! Verwijzingsbron niet gevonden.**a shows, by the dashed lines, the measured angular response of the dual polarized device in comparison to the simulated ones obtained in reception in Sec.II. We observe an excellent agreement between the simulated and the measured device angular responses (dots). Figure 6b shows the measured 2D angular response of the dual-polarized leaky design.

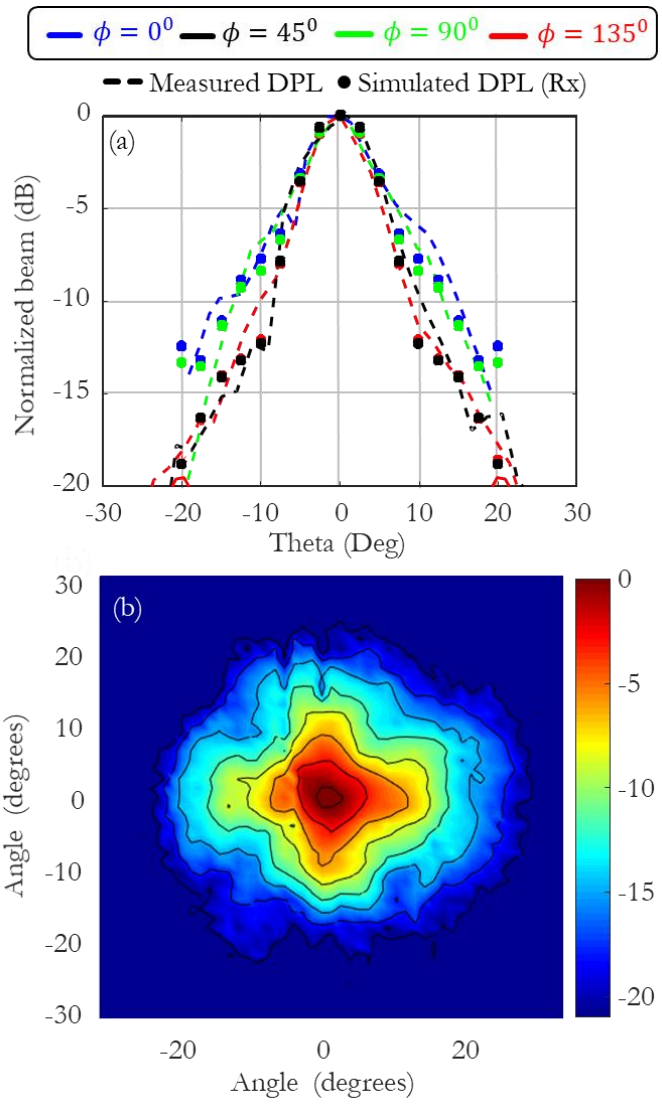

Fig. 6 (a) Comparison of the simulated and measured device angular responses obtained by the dual-polarized device, (b) the measured angular response shown on a 2D plane.

We next evaluate the normalized throughput of the dual-polarized device, $\frac{A\Omega}{\lambda^2}$. To this end, the sample chip has been mounted inside a stray-light tight setup, thermally anchored to the cold stage of an ADR (Adiabatic Demagnetization Cooler), operating at 120 mK. A blackbody radiator, whose temperature can be varied from 3 K up to 40 K, is used as an absolute calibration source. Eight mesh IR filters are used to define a THz band-pass with a center frequency of 1.55 THz and a bandwidth of 0.1 THz between the radiator and the detector. The details of this setup can be found in [20].

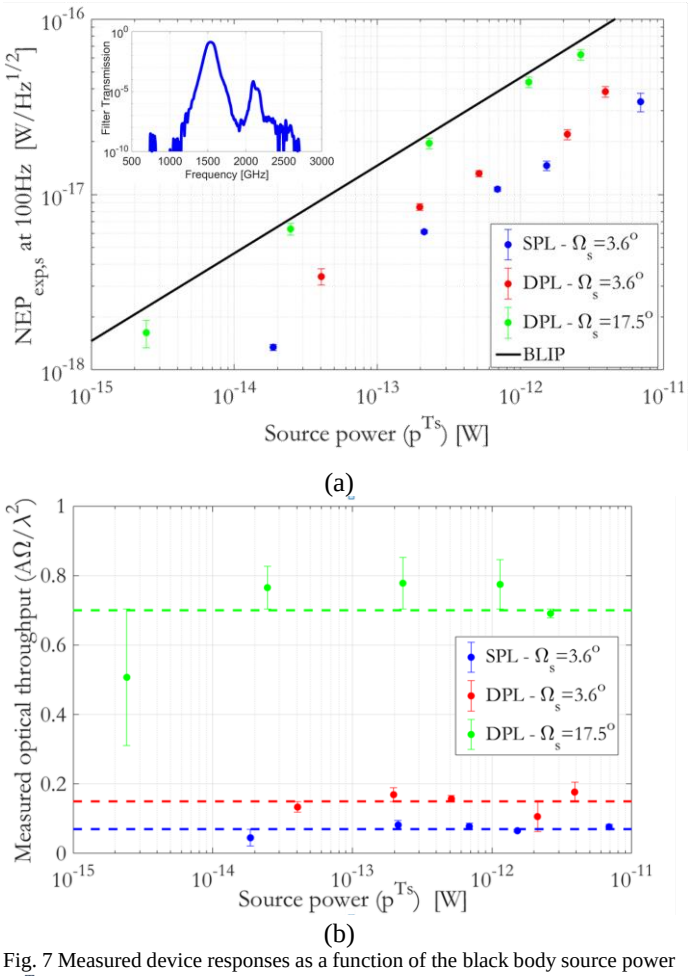

Fig. 7 Measured device responses as a function of the black body source power (p^{T_s}): (a) measured optical NEP ($NEP_{exp,s}$) at the output of the antenna. Since the NEP of the proposed devices is limited by the Poisson noise, a two times higher received power leads to a $\sqrt{2}$ higher NEP as in the case of the dual polarized device with respect to the single one in the same measurement setup ($\Omega_s = 3.6^o$). As a consequence, the SNR of the dual polarized device will be $\sqrt{2}$ higher than for the single polarized one. (b) The measured normalized optical throughputs ($A\Omega/\lambda^2$) of the single and dual-polarized devices.

At a distance of d = 35 mm from the test chip we have placed an aperture stop of a diameter D = 4.4 mm for recreating a small angle illumination (opening angle of $\Omega_s = 3.6^0$) and in a separate experiment, a stop with a D = 22 mm for recreating a large angle illumination (opening angle of $\Omega_s = 17.5$).

The device optical throughput, over a small bandwidth BW, centered around a frequency ν_0 can be derived from the experimental NEP, $NEP_{exp,s}$, similar to what is done in [4], as follows:

This article has been accepted for publication in a future issue of this journal, but has not been fully edited. Content may change prior to final publication. Citation information: DOI 10.1109/TTHZ.2018.2873890, IEEE Transactions on Terahertz Science and Technology

TABLE IV
SIMULATED AND MEASURED NORMALIZED OPTICAL THROUGHPUT ($A\Omega/\lambda^2$) OF THE EXPERIMENTAL SETUP AT 1.55 THZ

	Simulated		Measured	
	Single-polarized device	**Dual-polarized device**	**Single-polarized Device [11]**	**Dual-polarized Device**
3.6°	0.07	0.15	0.07±0.01	0.15±0.02
17.5°	-	0.64	-	0.7±0.08

$$\frac{A\Omega}{\lambda_0^2} = \frac{\int 2P^{T_S}(\nu)h\nu d\nu + \int \frac{4\Delta P^{T_S}(\nu)}{\eta_{pb}} d\nu}{NEP^2_{exp,s} - \int 2\left(P^{T_S}(\nu)\right)^2 d\nu} \quad (8)$$

where $P^{T_S}(\nu)$ is the spectral power emitted from the black body into two orthogonal polarized single modes multiplied with the transmission of our quasi-optical filters:

$$P^{T_S}(\nu) \approx B_s(\nu)\lambda^2 H(\nu) \quad (9)$$

Note that the second term in the denominator of (8), the wave noise, has very little effect for the current measurement conditions as difference from other experiments [23].

The experimental NEP is calculated from the measured device phase noise S_θ:

$$NEP_{exp}(f) = \frac{A\Omega}{\lambda_0^2} NEP_{exp,s}(f) \quad (10)$$

where

$$NEP_{exp,s}(f) = \sqrt{S_\theta(f)} \left(\frac{d\theta}{dp^{T_S}}\right)^{-1} \sqrt{1 + (2\pi f \tau_{qp})^2}. \quad (11)$$

and $p^{T_S} = \int P^{T_S}(\nu)d\nu$

The NEP_{exp} in (10) is evaluated at a single audio frequency high enough not to be limited by detector 1/f noise, and low enough not to be limited by the detector intrinsic time constant τ_{qp}.

Figure 7a shows the measured optical $NEP_{exp,s}$ referred at the output of the antenna as a function of the source power (9) for the three devices as well as the calculated NEP assuming background limited for single mode dual polarized radiation detection, (9), referred as NEP_{BLIP}. The filter stack transmission properties, $H(\nu)$, are shown in the figure inset. Figure 7a shows that the obtained $NEP_{exp,s}$ are higher for the dual polarized devices. Indeed, for the same measurement setup ($\Omega_s = 3.6deg$), the dual polarized device presents a $NEP_{exp,s}$ that is $\sqrt{2}$ higher than the one of the single polarized device, since it receives two times higher signal and the NEP is dominated by the Poisson noise [4]. As a consequence, the SNR of the dual polarized device will be $\sqrt{2}$ higher than for the single polarized one.

Using (8), we can extract the value of the measured normalized optical throughputs for different source temperatures. The values of the measured optical throughputs per source powers and their average values are shown in Fig. 7b for the three devices.

TABLE IV reports the average of these measured optical throughputs for several aperture sizes and the two considered devices. The measured results have an estimated 15% margin error due to the tolerances in the fabrication and measurement setup. The estimated values in Sec. II are also included in the table for comparison. Two important results can be emphasized from these results:

- Estimated normalized throughput values are in a very good agreement with the measured values.
- Measured normalized throughput from the dual polarized device is double than the one for the single-polarized device. This result experimentally proves a factor of two in the reception of two incoherent polarizations.

V. CONCLUSION

We have designed a dual polarized leaky wave antenna coupled MKID, operating at 1.55 THz, and compared it to its single polarized version. We have investigated, numerically and experimentally, the detector performance in terms of beam shape and optical throughput to an incoherent distributed source. Given the detection process is distributed over the KID resonator lines, the antenna has been evaluate numerically using CST in reception, and we have given the framework to evaluate the angular response and optical throughput from these simulations. We find that the aperture efficiency is a factor 2 higher for the dual polarized device. However the absence of air bridges in the fabricated device reduces the focusing efficiency due to the presence of additional modes in the detector. These modes can be suppressed by air bridges leading to basically a device that has twice the throughput of the single polarized version with the same angular selectivity.

We have measured the angular beam response and optical throughput of the fabricated the dual-polarized device at 1.55 THz. We find an excellent agreement between the measured and simulated angular responses as well as the normalized optical throughput values.

REFERENCES

[1] Farrah, D. et al. Review: Far-Infrared Instrumentation and Technology Development for the Next Decade. arXiv:1709.02389v1 (2017).
[2] P. K. Day, et al., "A broadband superconducting detector suitable for use in large arrays," *Nature*., vol. 425, pp. 817-821, Oct. 2003.
[3] Catalano, A. et al. Performance and calibration of the NIKA camera at the IRAM 30 m telescope. Astron. Astrophys. 569, A9 (2014).
[4] L. Ferrari, et al., "Antenna coupled KID performance verification for large format astrophysics arrays," *Transactions on Terahertz Science and Technology*., accepted for publication.

[5] J. J. A. Baselmans, et al., "A kilo-pixel imaging system for future space based far-infrared observatories using microwave kinetic inductance detectors," *Astronomy & Astrophysics*., vol. 601, pp. A89, May 2017.
[6] J. van Rantwijk, et al., "Multiplexed readout for 1000-pixel arrays of microwave kinetic inductance detectors," *IEEE Trans. on Microwave Theory and Techniques*., vol. 64, no. 6, pp. 1876-1883, Jun. 2016.
[7] Pastor, C. *et al.* "SAFARI optical system architecture and design concept." Proc. SPIE 9904, Space Telescopes and Instrumentation 2016: Optical, Infrared, and Millimeter Wave, 99043U: DOI: 10.1117/12.2232786; http://dx.doi.org/10.1117/12.2232786. July 2016
[8] A. Garufo, et al., "Radiation of logarithmic spiral antennas in the presence of dense dielectric lenses," *IEEE Trans. Antennas Propag*., No. 10, vol. 64, pp. 4168-4177, Jul. 2016.
[9] J. M. Edwards, et al., "Dual-polarized sinuous antennas on extended hemispherical silicon lenses," *IEEE Trans. Antennas Propag*., No. 9, vol. 60, pp. 4082-4091, Sep. 2012.
[10] R. O'Brient, et al., "A dual-polarized broadband planar antenna and channelizing filter bank for millimeter wavelengths," *Appl. Phys. Lett*., No. 6, vol. 102, DOI: 10.1063/1.4791692, pp. 26-32, Feb. 2013.
[11] A. Neto, et al., "Demonstration of the leaky lens antenna at submillimeter wavelengths," *Transactions on Terahertz Science and Technology*., Vol. 4, no. 1, pp. 26-32, Jan. 2014.
[12] J. Bueno, et al., "Full characterization of a background limited antenna coupled KID over an octave of bandwidth for THz radiation," *Appl. Phys. Lett*., vol. 11, Doi: 10.1063/1.4985060, 2017.
[13] O. Yurduseven, et al., "A dual-polarized leaky lens antenna for wideband focal plane arrays," *IEEE Trans. Antennas Propag*., No. 8, vol. 64, pp. 3330-3337, Aug. 2016.
[14] N. Llombart, et al., "Reception Power Pattern of Distributed Absorbers in Focal Plane Arrays: a Fourier Optics Analysis," *IEEE Trans. Antennas Propag*., doi: 10.1109/TAP.2018.2862359
[15] The homepage of CST Microwave Studio [Online]. Available: http://www.cst.com/
[16] Z. Chen, et al., "Fabrication and characterization of aluminum airbridges for superconducting microwave circuits," *Appl. Phys. Lett*., vol. 104, Doi: 10.1063/1.4863745, pp. 052602, 2014.
[17] D. Rutledge and S. Schwarz, "Planar multimode detector arrays for infrared and millimeter-wave applications," *IEEE Journal of Quantum Electronics*, vol. 17, no. 3, pp. 407-414, March 1981
[18] S. van Berkel, O. Yurduseven, A. Freni, A. Neto and N. Llombart, "THz Imaging Using Uncooled Wideband Direct Detection Focal Plane Arrays," in *IEEE Transactions on Terahertz Science and Technology*, vol. 7, no. 5, pp. 481-492, Sept. 2017.
[19] S. L. van Berkel, A. Garufo, N. Llombart and A. Neto, "A Quasi-Analytical Tool for the Characterization of Transmission Lines at High Frequencies [EM Programmer's Notebook]," in *IEEE Antennas and Propagation Magazine*, vol. 58, no. 3, pp. 82-90, June 2016.
[20] P. de Visser, et al., "Fluctuations in the electron system of a superconductor exposed to a photon flux," *Nature Communications*, vol. 5, DOI: 10.1038/ncomms 4130, Feb. 2014.
[21] Gao, J., Zmuidzinas, J., Mazin, B. A., Leduc, H. G. & Day, P. K. Noise properties of superconducting coplanar waveguide resonators. *Appl. Phys. Lett.* 90, 102507 (2007).
[22] R. Barends, et al., "Noise in NbTiN, Al, and Ta superconducting resonators on silicon and sapphire substrates," *IEEE Trans. Appl. Superconductivity*, Vol. 19, no. 3, pp. 936-939, Jun. 2009.
[23] D. Flanigan, et. al., "Photon noise from chaotic and coherent millimeter-wave sources measured with horn-coupled, aluminum lumped-element kinetic inductance detectors", Appl. Phys. Lett. 108, 083504 (2016); https://doi.org/10.1063/1.4942804

Ozan Yurduseven (S' 11 - M' 16) received the B.Sc. and M.Sc. (Hons.) degrees in Electronics and Communications Engineering from Yildiz Technical University, Istanbul, Turkey, in 2009 and 2011, respectively. He obtained his Ph.D. degree in Electrical Engineering, from Delft University of Technology, Delft, The Netherlands, in 2016.

His Ph.D. research was on the dev elopment of wideband integrated lens antennas for THz deep space investigation. During his Ph.D., he spent six months as a visiting researcher with the Instituto de Telecomunicações, Instituto Superior Técnico, Lisbon, Portugal, working on the development of double shell lens based integrated wideband sub-mm imaging systems. He has authored or co-authored over 40 publications in peer-reviewed journals and conferences. His current research interests include dielectric lens antennas for millimeter and sub-millimeter wave space applications, quasi-optical systems, numerical techniques in electromagnetics and metamaterials.

Dr. Yurduseven is a member of the IEEE Antennas and Propagation Society (IEEE APS) and the European Association on Antennas and Propagation (EurAPP). He received the Best Student Paper Award at the European Conference on Antennas and Propagation (EuCAP) in 2013 and was one of the co-authors of the conference proceeding that received Best Paper on Electromagnetism and Antenna Theory award in EuCAP 2016. He serves as a reviewer for IEEE TRANSACTIONS ON ANTENNAS AND PROPAGATION, IEEE TRANSACTIONS ON TERAHERTZ SCIENCE AND TECHNOLOGY and IEEE ANTENNAS AND WIRELESS PROPAGATION LETTERS.

Juan Bueno graduated in Physics from the University of Cantabria (Spain) in 2003 and received the Ph.D. degree at the University of Leiden (The Netherlands) in 2007. During his Ph.D. degree studies, he studied quantum crystals at very low temperatures. From 2007 to 2008, he was a postdoctoral fellow at the University of California, San Diego (USA) continuing his work on quantum crystals.

In 2008, he made the decision to switch research topics and interests from fundamental physics to the study of superconducting devices. He was awarded with a NASA Postdoctoral position (NPP), becoming a post doc at the Jet Propulsion Laboratory (USA) until 2010. During this time, he pioneered a new type of pair-breaking radiation detector, the Quantum Capacitance Detector. After his time at JPL, he joined the Center for Astrobiology (Spain) in 2010 after receiving a JAE-doc grant, working mainly on kinetic inductance detectors (KIDs). He became an instrument scientist in 2012 at SRON - Netherlands Institute for Space Research (The Netherlands), working on the development of KIDs for sub-mm wave and far IR space-based observatories.

Dr. Bueno has published more than 30 peer-reviewed papers, a third of them as the first author. His research interest concentrates on the development of ultra-sensitive broadband KIDs for future space-based missions.

Stephen Yates received a Ph.D. degree at the University of Bristol, Bristol, U.K., in 2003, working on experimental low temperature techniques for condensed matter physics.

He then worked at the CNRS-CRTBT Grenoble, France, as a Post-Doctoral Researcher on low temperature magnetism and superconductivity (2003-2004). He followed this also at CNRS-CRTBT with work on the development of low temperature detectors and techniques for astrophysics (2004-2006). He is currently an instrument scientist working on superconducting Microwave Kinetic Inductance Detectors (MKIDs) at SRON, the Netherlands Institute for Space Research, which he started in 2006. His current interests concentrate on MKID development for sub-mm applications but also include a wider interest in device physics and superconductivity, optical design, and full end to end instrument characterization and performance. Dr. Yates has published over 60 papers.

Andrea Neto (M'00–SM'10–F'16) received the Laurea degree (summa cum laude) in electronic engineering from the University of Florence, Florence, Italy, in 1994, and the Ph.D. degree in electromagnetics from the University of Siena, Siena, Italy, in 2000. Part of his Ph.D. degree was developed at the European Space Agency Research and Technology Center Noordwijk, The Netherlands.

He worked for the Antenna Section at the European Space Agency Research and Technology Center for over two years. From 2000 to 2001, he was a Postdoctoral Researcher with the California Institute of Technology, Pasadena, CA, USA, where he worked with the Sub-mm Wave Advanced Technology Group. From 2002 to January 2010, he was a Senior Antenna Scientist with TNO Defence, Security, and Safety, The Hague, The Netherlands. In February 2010, he became a Full Professor of

applied electromagnetism with the EEMCS Department, Technical University of Delft, Delft, The Netherlands, where he formed and leads the THz Sensing Group. His research interests include the analysis and design of antennas with an emphasis on arrays, dielectric lens antennas, wideband antennas, EBG structures, and THz antennas.

Dr. Neto served as an Associate Editor of the IEEE TRANSACTIONS ON ANTENNAS AND PROPAGATION (2008–2013) and IEEE ANTENNAS AND WIRELESS PROPAGATION LETTERS (2005–2013). He is a member of the Technical Board of the European School of Antennas and organizer of the course on antenna imaging techniques. He is a member of the Steering Committee of the Network of Excellence NEWFOCUS, dedicated to focusing techniques in mm and sub-mm wave regimes. In 2011, he was the recipient of the European Research Council Starting Grant to perform research on Advanced Antenna Architectures for THz Sensing Systems. He was the recipient of the H. A. Wheeler Award for the best applications paper of 2008 in the IEEE TRANSACTIONS ON ANTENNAS AND PROPAGATION, the Best Innovative Paper Prize of the 30th ESA Antenna Workshop in 2008, and the Best Antenna Theory Paper Prize of the European Conference on Antennas and Propagation (EuCAP) in 2010. In 2011, he was the recipient of the European Research Council Starting Grant to perform research on advanced antenna architectures for THz sensing systems.

Jochem Baselmans (1974) is senior instrument scientist at the SRON Netherlands Institute for Space Research where he works since 2002 within the Technology division. He is also, since 2015, Associate professor in the THz sensing group at Delft University of Technology. He graduated in 1998 on at the University of Groningen and received his PH.D. (summa cum laude) at the university of Groningen on 2002, entitled: 'Controllable Josephson Junctions'. He started in 2002 as post-doctoral Instrument Scientist at SRON Netherlands Institute for Space Research where has worked until 2004 on Hot Electron Bolometer mixers. In 2005 he moved to SRON Utrecht and started working on Microwave Kinetic Inductance Detectors, after a 3 month visit to the California Institute of Technology, Pasadena, USA. He now leads the Dutch effort on the development of Microwave Kinetic Inductance Detectors, where his main interests are ultra-sensitive MKIDs for THz radiation detection and advanced on-chip imaging spectrometers for sub-THz imaging spectroscopy. In 2015 Jochem Baselmans received an ERC Consolidator grant to develop an advanced imaging spectrometer based upon MKIDs. Dr. Baselmans published in excess of 100 papers.

Nuria Llombart (S'06–M'07–SM'13) received the Master's degree in electrical engineering and Ph.D. degrees from the Polytechnic University of Valencia, Valencia, Spain, in 2002 and 2006, respectively.

During her Master's degree studies, she spent one year at the Friedrich-Alexander University of Erlangen-Nuremberg, Erlangen, Germany, and worked at the Fraunhofer Institute for Integrated Circuits, Erlangen, Germany. From 2002 to 2007, she was with the Antenna Group, TNO Defence, Security and Safety Institute, The Hague, The Netherlands, working as a Ph.D. student and afterwards as a Researcher. From 2007 to 2010, she was a Postdoctoral Fellow with the California Institute of Technology, working with the Submillimeter Wave Advance Technology Group, Jet Propulsion Laboratory, Pasadena, CA, USA. She was a "Ramón y Cajal" fellow in the Optics Department, Complutense University of Madrid, Madrid, Spain, from 2010 to 2012. In September 2012, she joined the THz Sensing Group, Technical University of Delft, Delft, The Netherlands, where as of February 2018 she is a Full Professor. She has coauthored more than 150 journal and international conference contributions. Her research interests include the analysis and design of planar antennas, periodic structures, reflector antennas, lens antennas, and waveguide structures, with emphasis in the THz range.

Dr. Llombart was the recipient of the H. A. Wheeler Award for the Best Applications Paper of 2008 in the IEEE TRANSACTIONS ON ANTENNAS AND PROPAGATION, the 2014 THz Science and Technology Best Paper Award of the IEEE Microwave Theory and Techniques Society, and several NASA awards. She was also the recipient of the 2014 IEEE Antenna and Propagation Society Lot Shafai Mid-Career Distinguished Achievement Award. She serves as a Board member of the IRMMW-THz International Society. In 2015, she was the recipient of European Research Council Starting Grant.